The Modified Bidomain Model with Diffusive Inclusions

Yves Coudière, Anđela Davidović, Clair Poignard

The Modified Bidomain Model with Diffusive Inclusions

Yves Coudière[1,2,3,4], Anđela Davidović[1,2,3,4] (andjela.davidovic@inria.fr) and Clair Poignard[1,2,3]

[1]INRIA Bordeaux Sud-Ouest, [2]University Bordeaux, [3]Institut de Mathématiques de Bordeaux (IMB), [4]IHU-Liryc

The standard bidomain model

- Widely accepted model
- Very good for the healthy tissues

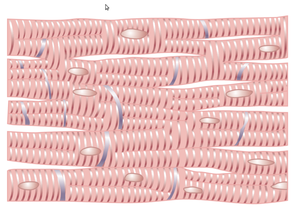

Figure: The patch of the cardiac tissue [4].

- Derived from the microscopic problem
- Assumptions used
  - periodicity
  - uniformly distributed ECM
  - anisotropic conductivities

Drawbacks - Examples

- There are non-small regions where myocytes are not present
- The **laminar structure**

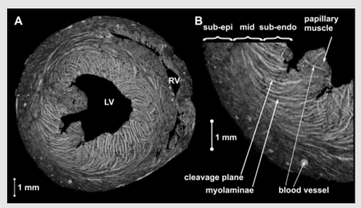

Figure: The laminar structure of myocardium. [2]

- The **infarct border zone**.

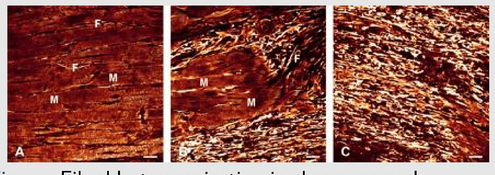

Figure: Fibroblast organization in sheep: normal ventricular myocardium (A), infarct border zone (B) and centre (C), 1 week after infarction. [3]

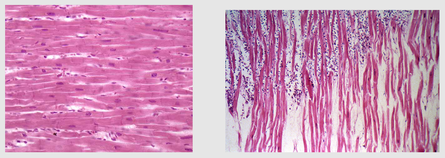

Figure: Normal tissue and Myocardial infarction in human. Tissue histology.

Modelling assumptions

- Periodic diffusive inclusions of size ε.
- Isotropic conductivity in the inclusions.
- No cells in the inclusions. Passive conductors.
- Standard transmission conditions.

Microscale model

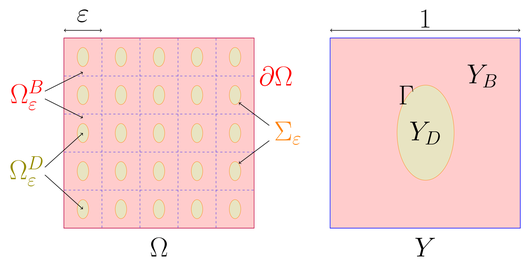

- Bidomain model

$$\begin{aligned}
\partial_t h_\varepsilon + g(v_\varepsilon, h_\varepsilon) &= 0, && \text{in } \Omega_\varepsilon^B,\\
\partial_t v_\varepsilon + I_{ion}(v_\varepsilon, h_\varepsilon) &= \nabla\cdot(\sigma_\varepsilon^i \nabla u_\varepsilon^i), && \text{in } \Omega_\varepsilon^B,\\
\partial_t v_\varepsilon + I_{ion}(v_\varepsilon, h_\varepsilon) &= -\nabla\cdot(\sigma_\varepsilon^e \nabla u_\varepsilon^e), && \text{in } \Omega_\varepsilon^B.
\end{aligned}$$

  - intra- and extra-cellular conductivities σ_ε^i and σ_ε^e
  - unknown potentials u_ε^i and u_ε^e
  - transmembrane potential $v_\varepsilon := u_\varepsilon^i - u_\varepsilon^e$
  - $I_{ion}(v,h)$ and $g(v,h)$ define specific ionic model
- Diffusive inclusions

$$\nabla\cdot(\sigma_\varepsilon^d \nabla u_\varepsilon^d) = 0, \qquad \text{in } \Omega_\varepsilon^D.$$

  - conductivity σ_ε^d
  - unknown potential u_ε^d
- Interface

$$\left.\begin{aligned}
\sigma_\varepsilon^i \nabla u_\varepsilon^i\cdot \mathbf{n}_{\Sigma_\varepsilon} &= 0,\\
\sigma_\varepsilon^e \nabla u_\varepsilon^e\cdot \mathbf{n}_{\Sigma_\varepsilon} &= \sigma_\varepsilon^d \nabla u_\varepsilon^d\cdot \mathbf{n}_{\Sigma_\varepsilon},\\
u_\varepsilon^e &= u_\varepsilon^d,
\end{aligned}\right| \qquad \text{on } \Sigma_\varepsilon.$$

Method: Homogenisation

- Assume:

$$u_\varepsilon^i(t,x) = u_0^i(t,x) + u_1^i(t,x,\frac{x}{\varepsilon}) + \cdots,$$
$$u_\varepsilon(t,x) = u_0(t,x) + u_1(t,x,\frac{x}{\varepsilon}) + \cdots.$$

- Let $\varepsilon \to 0$. Derive the homogenised problem and the cell problems.
- According to [1], *a priori* estimates ensure the two–scale convergence

Limit macroscale model

- The limit problem in whole Ω:

$$\begin{aligned}
\partial_t h_0 + g(v_0, h_0) &= 0,\\
|Y_B|(\partial_t v_0 + I_{ion}(v_0, h_0)) &= \nabla\cdot(\tilde\sigma_i \nabla u_0^i),\\
|Y_B|(\partial_t v_0 + I_{ion}(v_0, h_0)) &= -\nabla\cdot(\tilde\sigma_e \nabla u_0).
\end{aligned}$$

- New conductivities

$$\tilde\sigma_i = \sigma^i|Y_B| + A^i(\sigma_i, w^i),$$
$$\tilde\sigma_e = \sigma^e|Y_B| + \sigma^d|Y_D| + A(\sigma_e, \sigma_d, w)$$

  where A_i and A are matrices obtained by solving the cell problems on Y for unknown functions w^i and w.

Remarks:

- The conductivities depend on the volume fraction and on the geometry of the diffusive part.
- If $\sigma_e = \sigma_d$ then on the volume fraction only.
- If $|Y_D| = 0$ it is the standard bidomain model.
- If $|Y_B| = 0$ it is only the diffusion model.

Numerical results

- *FreeFem++* and *gnuplot*.
- Mitchell Schaeffer ionic model.
- 2D simulations on Ω rectangle, SBDF2 numerical scheme.
- Simple shapes of inclusions (circles and ellipses).

Table: The values of the new conductivities depending on the diffusion inclusions [10^{-1}S/m]. The first row: values for the standard bidomain model, without inclusions.

geometry	vol frac	σ^d	$\sigma^*_{i_{11}}$	$\sigma^*_{i_{22}}$	$\sigma^*_{e_{11}}$	$\sigma^*_{e_{22}}$
-	-	-	1.74	0.19	3.9	1.97
circle	0.18	3	1.29	0.18	3.28	2.45
ellipse (1:4)	0.18	3	0.31	0.19	0.75	2.61
circle	0.2	3	1.26	0.17	3.29	2.53
ellipse (1:1.5)	0.2	3	1.13	0.18	2.82	2.58
ellipse (1:2)	0.2	3	0.86	0.18	2.09	2.64
circle	0.4	3	1.07	0.15	3.42	3.53
ellipse (1:1.5)	0.4	3	0.81	0.16	2.53	3.70
circle	0.7	3	0.69	0.09	5.08	7.89

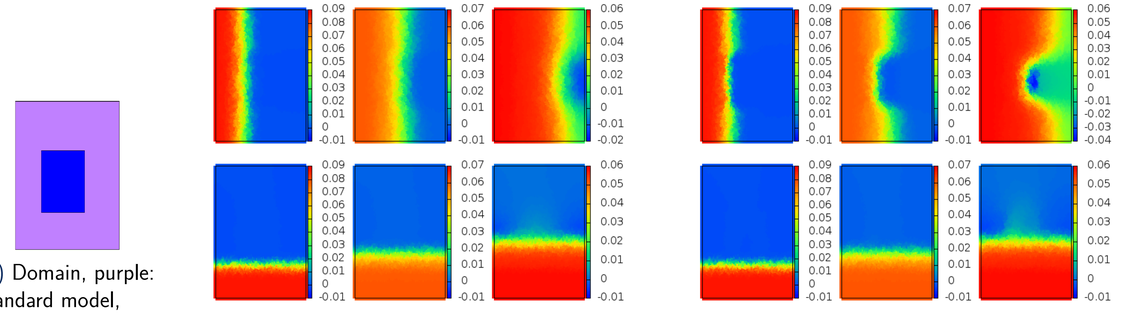

(a) Domain, purple: standard model, blue: modified. (b) Circular inclusions. (c) Elliptical inclusions. Axes length ratio 1:4.

Figure: Simulation of the standard bidomain with the "scar patch". $\sigma^d = 3$, volume fraction 0.18, comparing inclusions geometries.

Conclusions

- Inclusions change the speed of propagation and depending on geometry, the anisotropy ratio.
- Rigorous and practical way to link the structural disease to macroscopic conductivities.

Future work

- Use the late enhancement MRI for the volume fraction of the extracellular space.
- Cells in the additional ECM. Boundary conditions.

References

[1] Allaire, Gregoire. "Homogenization and two-scale convergence." SIAM Journal on Mathematical Analysis 23.6 (1992): 1482-1518.

[2] Gilbert, Stephen H., et al. "Visualization and quantification of whole rat heart laminar structure using high-spatial resolution contrast-enhanced MRI." American Journal of Physiology-Heart and Circulatory Physiology 302.1 (2012): H287-H298.

[3] Camelliti, Patrizia, Thomas K. Borg, and Peter Kohl. "Structural and functional characterisation of cardiac fibroblasts." Cardiovascular research 65.1 (2005): 40-51.

[4] Hall, John E. Guyton and Hall Textbook of Medical Physiology: Enhanced E-book. Elsevier Health Sciences, 2010.